



1 **Highly Viscous Phase Behavior of Organic-Rich Urban**

2 **PM_{2.5}**

3 Atta Ullah¹, Ji Yi Lee², Zhijun Wu³, Kyoung-Soon Jang⁴, Mijung Song^{1,5}

4 ¹Department of Earth and Environmental Sciences, and Earth Environmental System Research Center, Jeonbuk
5 National University, Jeollabuk-do Jeonju-si 54896, Republic of Korea; ²Department of Environmental Science
6 & Engineering, Ewha Womans University, Seoul 03760, Republic of Korea; ³State Key Joint Laboratory of
7 Environmental Simulation and Pollution Control, College of Environmental Sciences and Engineering, Peking
8 University, Beijing 100871, China; ⁴Bio-Chemical Analysis Team, Korea Basic Science Institute, Cheongju
9 28119, Republic of Korea; ⁵Department of Environment and Energy, Jeonbuk National University, Jeollabuk-do
10 Jeonju-si 54896, Republic of Korea

11 *Correspondence to:* Mijung Song (Mijung.Song@jbnu.ac.kr)



12 Abstract

13 Atmospheric aerosol viscosity strongly influences particle phase state, internal mixing, and multiphase chemical
14 processes, yet direct quantitative constraints for ambient urban PM_{2.5} remain limited. Here, we investigated the
15 phase behavior and viscosity of organic-rich PM_{2.5} samples collected during autumn 2023 from the urban
16 environments of Seoul and Beijing. Using filter extracts, relative humidity (RH)-dependent phase transitions and
17 morphological evolution of the droplets were examined by optical microscopy, revealing frequent two-phase and
18 three-phase morphologies during dehydration. Aerosol viscosity was quantitatively constrained at ~290 K under
19 experimentally accessible RH condition ($\leq \sim 40\%$) using the poke-and-flow technique coupled with fluid-dynamic
20 simulations, yielding viscosities spanning from $\sim 10^4$ to $> \sim 10^8$ Pa·s. Compared with previously reported
21 laboratory-based viscosity measurements, the inferred viscosities of ambient PM_{2.5} were comparable to or
22 exceeded those reported for organic-rich ternary systems (i.e., sucrose–AS–H₂O), that are commonly used as
23 laboratory proxy systems in aerosol viscosity studies. These results indicate that organic-rich urban PM_{2.5} can
24 exhibit highly viscous, semisolid to non-flowing behavior and provide quantitative, field-based, compositionally
25 constrained viscosity data for urban aerosols.

26 Keyword: Viscosity, Morphology, PM_{2.5}, Organic Aerosol, Northeast Asia.



27 1. Introduction

28 Atmospheric fine particulate matter (PM_{2.5}) in urban megacities undergoes a range of general physicochemical
29 processes, including hygroscopic growth, phase transitions, viscosity changes, and diffusion-limited internal
30 mixing, which are strongly modulated by relative humidity (RH) (Swietlicki et al., 2008; Guo et al., 2014; Reid
31 et al., 2018; Song et al., 2022; Freedman et al., 2024; Tan et al., 2024). These processes play a critical role in gas–
32 particle partitioning (Zuend and Seinfeld, 2012; Zhou et al., 2013; Gkatzelis et al., 2018; Zaveri et al., 2020),
33 heterogeneous chemical reactivity (Li et al., 2020; Rasool et al., 2023; Song et al., 2025), aging dynamics
34 (Shiraiwa et al., 2011; Liu et al., 2025), and cloud nucleation potential (Suda et al., 2014; Cheung et al., 2020;
35 Pöhlker et al., 2023), yet their underlying mechanisms remain poorly constrained by empirical observations. This
36 limitation fundamentally undermines the accurate parametrization of urban aerosol impacts within the regional
37 and global atmospheric models.

38 PM_{2.5} exerts major influences on air quality, human health, and climate forcing because of its chemical
39 complexity and diverse physical properties (Seinfeld et al., 2016; McNeill, 2017; Su et al., 2020; Nault et al., 2021;
40 Wall et al., 2022; El Haddad et al., 2024; Bei et al., 2025; Manavi et al., 2025; Sun et al., 2025). PM_{2.5} typically
41 consists of organic aerosols (OA), inorganic species, elemental or black carbon (EC/BC), sea salt, and trace metals.
42 Among these components, OA, including primary (POA) and secondary (SOA), have been frequently observed
43 as the dominant fraction across many continental regions, accounting for approximately 20–90 % of total PM_{2.5}
44 mass (Kanakidou et al., 2005; Hallquist et al., 2009; Jimenez et al., 2009; Huang et al., 2014; Zhang et al., 2017;
45 Jeon et al., 2023). These OA are chemically complex, encompassing thousands of molecules, and their oxygen-
46 to-carbon elemental ratios (O:C) have been shown to vary with atmospheric processing and environmental
47 conditions (Zhang et al., 2007; Aiken et al., 2008; Canagaratna et al., 2015; An et al., 2019; Daellenbach et al.,
48 2019; Sun et al., 2025; Cai et al., 2026).



49 Among the physical properties affected by the chemical complexity and atmospheric evolution of PM_{2.5},
50 viscosity is particularly important for controlling particle phase state and reactivity. Viscosity is the internal
51 resistance of a material to flow or deformation, quantifying the molecular mobility within a condensed phase. In
52 the atmospheric context, viscosity serves as a critical indicator of particle phase state: aerosols with viscosities
53 below 10² Pa·s behave as liquids, those between 10² and 10¹² Pa·s are semisolids, and particles exceeding 10¹²
54 Pa·s are solids (Koop et al., 2011; Zobrist et al., 2011). Variations in viscosity can dictate how rapidly molecules
55 diffuse, mix, and react within aerosol particles. A highly viscous particle restricts internal diffusion and slows
56 multiphase chemistry, whereas low-viscosity liquid particles facilitate rapid gas–particle exchange and aging
57 (Kuwata and Martin, 2012; Berkemeier et al., 2014; Gou et al., 2025).

58 During the past decade, extensive laboratory studies have attempted to quantify aerosol viscosity using organic
59 or mixed organic–inorganic systems (Renbaum-Wolff et al., 2013a; Song et al., 2016b; Freedman, 2017; Marshall
60 et al., 2018; Rovelli et al., 2019; Jeong et al., 2022; Tong et al., 2022; Mahant et al., 2023; Sheldon et al., 2023;
61 Gou et al., 2025). Measurements for SOA derived from anthropogenic (i.e., toluene, diesel fuel vapors, and
62 phenolic compounds) and biogenic (i.e., isoprene, α -pinene, β -ocimene, limonene, β -caryophyllene, valencene,
63 and farnesene isomer mixture) precursors have revealed that viscosity can span more than ten orders of magnitude,
64 from 10⁻³ Pa·s under humid conditions to over \sim 10⁸ Pa·s at low RH (Renbaum-Wolff et al., 2013b; Grayson et
65 al., 2016; Hinks et al., 2016; Song et al., 2016a; Song et al., 2019; Ullmann et al., 2019; Maclean et al., 2021;
66 Smith et al., 2021; Nikkho et al., 2024; Liu et al., 2026). These findings demonstrate that aerosol viscosity depends
67 strongly on chemical composition, including the organic-to-inorganic mass ratio (OIR), RH, and temperature.
68 However, almost all such data have been derived from laboratory-generated SOA or proxy mixtures, rather than
69 real ambient particles.

70 Seoul and Beijing represent typical urban environments influenced by mixed anthropogenic emissions, where
71 PM_{2.5} is frequently dominated by OA and secondary inorganic aerosols (SIA) (Son et al., 2012; Tao et al., 2017;



72 Kim et al., 2018; Zhou et al., 2020; Kim et al., 2022; Qiu et al., 2023; Cheng et al., 2024b; Daellenbach et al.,
73 2024). Field studies have shown that OA frequently contributes more than half of the PM_{2.5} mass in Seoul and
74 Beijing and comprises a mixture of POA (traffic, cooking, biomass, or coal/solid-fuel combustion) and SOA
75 formed from various precursors under a range of meteorological conditions (Sun et al., 2010; Hu et al., 2017; Kim
76 et al., 2017; Zhao et al., 2019; Qiu et al., 2023; Cheng et al., 2024b). In such OA-rich urban environments, the
77 phase state and viscosity of PM_{2.5} are expected to be strongly controlled by the properties of the organic fraction,
78 with direct implications for hygroscopic growth, gas–particle partitioning, and particle diffusion (Shiraiwa et al.,
79 2011; Davies and Wilson, 2015; Hosny et al., 2016; Tong et al., 2022). Consequently, direct constraints on the
80 phase state and viscosity of urban OA-containing PM_{2.5} remain essential for interpreting PM_{2.5} composition and
81 reducing uncertainties in process-level air-quality assessments.

82 In this study, PM_{2.5} samples were collected from the urban environments of Seoul and Beijing during autumn
83 2023. The samples were characterized by high organic mass fractions, representing organic-rich urban aerosols.
84 Using filter extracts, we investigated RH-dependent phase behavior and morphological evolution using optical
85 microscopy. We then quantitatively constrained aerosol viscosity at a temperature of ~290 K under experimentally
86 accessible RH conditions ($\leq \sim 40\%$) using the poke-and-flow technique. Finally, we compared the determined
87 viscosities with those reported in previous laboratory studies of organic–inorganic aerosol systems. By providing
88 direct quantitative viscosity data for field-collected PM_{2.5} in urban environments, this work advances our
89 understanding of the physicochemical behavior of ambient aerosols in the real atmosphere.

90 2. Experimental and methods

91 2.1 Measurement sites and collection of PM_{2.5} samples

92 PM_{2.5} sampling was conducted at an urban environmental monitoring station in Bulgwang-dong, Seoul (37.61°
93 N, 126.93° E) and the Changping campus of Peking University, Beijing (40.25°N, 116.19°E). Both sites are
94 located in densely populated metropolitan areas characterized by heavy traffic and significant industrial activity,



95 making them representative of typical urban environments. At each site, a total of three PM_{2.5} samples were
96 collected on quartz-fiber filters (8 × 10 in., Pall Corporation, 7204) over the sampling period between September
97 and October 2023. Each sample was collected from 10:00 to 09:00 local time using a high-volume sampler
98 operating at approximately 1000 L min⁻¹ (SIBATA HV-1000R, Japan). During the sampling period, the average
99 ambient RH and temperature were 69 ± 12 % and 290 ± 4 K at the Seoul site, and 54 ± 13 % and 293 ± 4 K at the
100 Beijing site, respectively. After collection, filters were stored at a temperature of ~255 K for subsequent analysis
101 within ~1 month. For the morphology (Sect. 2.2) and viscosity (Sect. 2.3) experiments, PM_{2.5} droplets prepared
102 from each PM_{2.5} filter extract, as detailed in Sect. S2, were deposited onto a hydrophobic glass substrate (Hampton
103 Research, Canada) using a nebulizer (MEINHARD, PerkinElmer, USA). Details of the methods used to determine
104 chemical compositions are provided in Sect. S1 of the Supplementary Information. Table 1 also summarizes the
105 sampling information and the chemical composition of the six PM_{2.5} samples.

106 **2.2 Observation of morphological change upon dehydration**

107 To investigate morphological changes of the PM_{2.5} droplets on a hydrophobic substrate, optical microscopy was
108 employed following the approach used in previous studies (Ham et al., 2019; Jeong et al., 2022; Song et al., 2022;
109 Seong et al., 2024; Song et al., 2025). In brief, before the experiment, the PM_{2.5} droplets were equilibrated at
110 ~100% RH and 290 ± 1 K for ~20 min, and then the RH was reduced at a rate of 0.5 % RH min⁻¹ in an RH and
111 temperature-controlled flow cell (TSA12Gi, Instec, USA) down to ~0% RH. During typical experiments, the
112 morphological evolution of the droplets before, during, and after poking was monitored via optical microscopy
113 (Olympus BX43, 40× objective, Japan) and recorded with a CCD camera (DigiRetina 16, Tucsen, China). The
114 RH sensor within the flow cell was calibrated at 290 ± 1 K using deliquescence relative humidity of K₂CO₃ (44%
115 RH), NaCl (76% RH), and (NH₄)₂SO₄ (80% RH), with an associated uncertainty of ±1.5%. RH control was
116 achieved by adjusting the mixing ratio of dry N₂ and saturated H₂O vapor, while maintaining a constant total flow



117 rate of 500 sccm. The experimental temperature (290 ± 1 K) was selected to closely reflect the average conditions
118 at the sampling sites, thereby ensuring environmental relevance.

119 **2.3 Poke-and-Flow technique coupled with fluid simulations**

120 The poke-and-flow technique was employed to determine the viscosity of highly viscous $PM_{2.5}$ droplets on a
121 hydrophobic substrate within a temperature- and RH-controlled flow cell (Grayson et al., 2015; Song et al., 2015;
122 Song et al., 2025). Droplets (~ 20 – 40 μm in diameter) prepared from $PM_{2.5}$ filter extract were deposited onto a
123 hydrophobic glass substrate and conditioned in the flow-cell. Their morphological evolution before, during, and
124 after poking was monitored using optical microscopy (Olympus CKX53 with a $40\times$ objective, Japan) and recorded
125 with a CCD camera (Hamamatsu, C11440-42U30, Japan). For viscosity measurements, droplets were first
126 equilibrated at $\sim 100\%$ RH, then RH was decreased to $\sim 40\%$ at $\sim 1\%$ RH min^{-1} . Poking was performed at RH levels
127 of $\sim 40\%$, $\sim 30\%$, $\sim 20\%$, $\sim 10\%$, and $\sim 0\%$ using a fine needle (Jung Rim Medical Industrial, South Korea) mounted
128 on a micromanipulator (Narishige, model MO-152, Japan) to identify the critical RH for particle cracking. Before
129 each poking, droplets were conditioned for ~ 1 h at the target RH to ensure equilibration (Sect. S4), consistent with
130 previous studies on semisolid particles (Kiland et al., 2023; Gerrebos et al., 2024). Following poking, a hole
131 formed and gradually closed; the time required for the hole to recover 50% of its initial diameter was defined as
132 the experimental flow time, $\tau_{(exp, flow)}$. In typical experiments, one to five particles per sample were analyzed at
133 each RH. At RH $> \sim 40\%$, the $PM_{2.5}$ droplets behaved as low-viscosity liquids and rapidly relaxed upon poking,
134 resulting in immediate hole closure and the absence of a well-defined $\tau_{(exp, flow)}$. As a result, the poke-and-flow
135 method was not suitable for quantitatively constraining viscosity under these high-RH conditions.

136 Viscosities were then determined from $\tau_{(exp, flow)}$ using finite-element fluid flow simulations in COMSOL
137 Multiphysics, following established methods (Renbaum-Wolff et al., 2013b; Grayson et al., 2015; Song et al.,
138 2015; Song et al., 2016a) detailed in Sect. S3. Model parameters, including slip length, surface tension, contact
139 angle, and density, are summarized in Table S2. Viscosity was iteratively adjusted until the simulated flow time



140 $\tau_{(model, flow)}$ matched $\tau_{(exp, flow)}$. At low RH, droplets exhibited brittle cracking without relaxation, indicating non-
141 flowing behavior. If no recovery occurred over 2 h, a lower-bound viscosity of $\sim 1 \times 10^8$ Pa·s was assigned
142 (Renbaum-Wolff et al., 2013b; Jeong et al., 2022; Gerrebos et al., 2024; Gerrebos et al., 2025).

143 3. Results and discussion

144 3.1 Chemical characteristics of PM_{2.5}

145 The chemical composition of PM_{2.5} collected from Seoul and Beijing during autumn 2023 is summarized in Fig.
146 S2 and Table 1. The major components include organic matter (OM), sulfate, nitrate, ammonium, and minor ions
147 (e.g., K⁺, Na⁺, Ca²⁺, Mg²⁺, and Cl⁻). OM consistently accounted for more than ~65% of the total PM_{2.5} mass across
148 all the samples. Although this classification captures the dominant aerosol constituents, trace species such as
149 metals, black carbon, and crustal materials also contribute to PM_{2.5} but were not the focus of this study.

150 The daily PM_{2.5} concentrations at the Seoul and Beijing sites ranged from ~7.0 to 31.7 $\mu\text{g m}^{-3}$, encompassing
151 both relatively clean and polluted conditions based on the World Health Organization (WHO) 24-hour air quality
152 guideline of 15 $\mu\text{g m}^{-3}$ (World Health Organization, 2021). Over this range, the OIR varied from approximately
153 2:1 to 8:1, consistent with values commonly observed in various tropospheric environments (Hodzic et al., 2020;
154 Cheng et al., 2024a; Zhang et al., 2024).

155 The bulk O:C ratios (~0.4 – 0.5 at both sites, Table 1) fall within the typical range for urban OA (Aiken et al.,
156 2008; Chen et al., 2015; Zhou et al., 2020), indicating that the organics were overall moderately oxidized. This
157 composition suggests a substantial fraction of hydrophilic, highly oxygenated secondary organics alongside a non-
158 negligible pool of more hydrophobic, less oxidized material (Kim et al., 2025). Consequently, autumn-time OM
159 in Seoul and Beijing can be characterized as an amphiphilic mixture, consistent with previous mass spectrometric
160 observations of urban aerosols in the region (Kim et al., 2022). Although inorganic ions were not the dominant
161 mass component as reflected by the OIR ranges (Table 1), they still represented an important fraction of PM_{2.5},



162 primarily as SIA dominated by ammonium sulfate (AS) with additional contributions from ammonium nitrate
163 (AN) (Fig. S2; Sect. S1).

164 **Table 1.** Summary of mean ambient temperature, relative humidity (RH), mass concentration of PM_{2.5}, and
165 sulfate, nitrate, ammonium, and minor ions (K⁺, Na⁺, Ca²⁺, Mg²⁺, and Cl⁻) in Seoul and Beijing. The mean
166 concentration of organic material (OM) was determined by deducing the inorganic components, including sulfate,
167 nitrate, ammonium, and minor ions, from the PM_{2.5} mass concentration. OIR refers to the organic-to-inorganic
168 mass ratio, whereas O:C means oxygen-to-carbon elemental ratio.

Sampling date (mm/dd)	Ambient temperature (K)	Ambient RH (%)	PM _{2.5} μg/m ⁻³	SO ₄ ²⁻ μg/m ⁻³	NO ₃ ⁻ μg/m ⁻³	NH ₄ ⁺ μg/m ⁻³	Minor μg/m ⁻³	OM μg/m ⁻³	OIR	O:C
Seoul										
09/30	291 ± 4	76 ± 6	16.8	2.2	0.6	0.9	0.3	12.9	3:1	0.45
10/12	290 ± 6	62 ± 13	16.4	1.9	1.0	1.0	0.2	12.3	3:1	0.47
10/15*	287 ± 4	84 ± 6	23.0	3.2	2.2	1.6	0.5	15.5	2:1	0.45
Beijing										
09/21	296 ± 2	61 ± 8	16.5	1.3	0.3	0.3	0.1	14.6	8:1	0.50
10/03	293 ± 3	61 ± 6	31.7	2.5	3.7	1.5	0.7	23.1	3:1	0.48
10/14*	289 ± 5	47 ± 15	7.0	1.0	0.7	0.3	0.3	4.7	3:1	0.52

*Data from Song et al. (2025).

169 170 3.2 Morphological characteristics and phase behavior of PM_{2.5} droplets

171 To directly observe the phase behavior under progressively lowering RH, micrometer-sized droplets generated
172 from PM_{2.5} extracts were monitored in a temperature- and RH-controlled flow-cell at 290 ± 1 K. This temperature
173 closely matches the mean ambient conditions during the autumn sampling period at both sites (Seoul: 291 ± 6;
174 Beijing: 291 ± 4 K; Table 1). Figure 1 shows optical images at four RH levels (~95 %, ~85 %, ~60 %, and ~20
175 %), illustrating the evolution of particle morphology and phase state during dehydration. At high RH (~95 %),
176 droplets behaved as homogeneous single-liquid particles. They appeared smooth and rounded, with uniform



177 optical contrast and no discernible internal structure, indicating that near water saturation, the urban PM_{2.5} extracts
178 form well-mixed single liquid droplets.

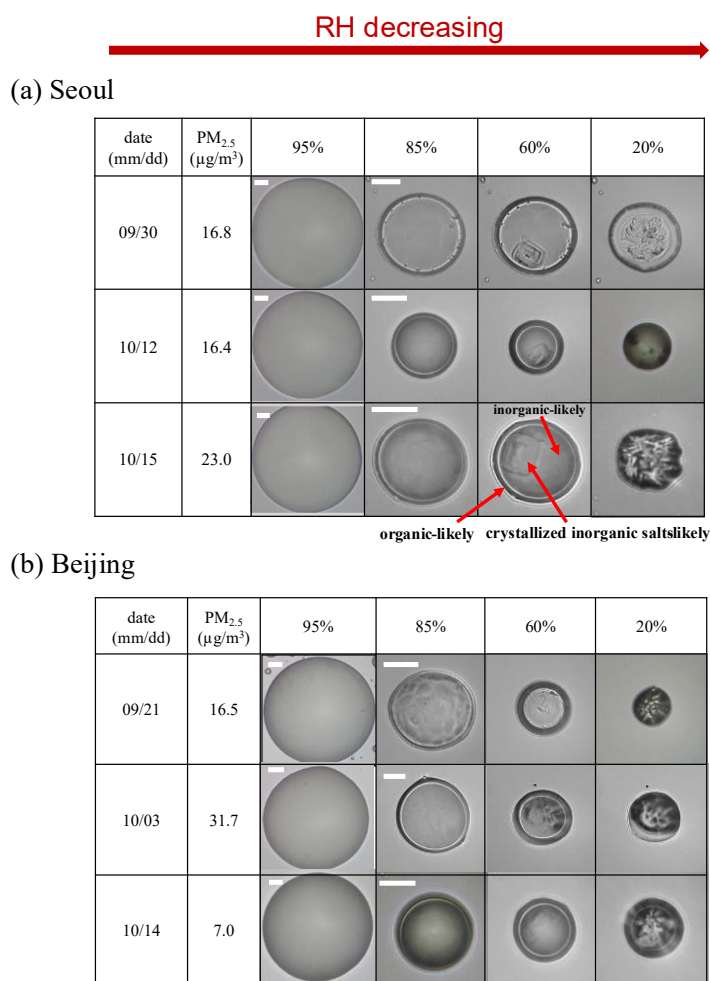
179 As RH decreased to ~85 %, all droplets exhibited internal structuring consistent with liquid-liquid phase
180 separation (LLPS) (Ciobanu et al., 2009; Song et al., 2012; Freedman, 2017; Ham et al., 2019; Lam et al., 2021;
181 Freedman et al., 2024). Distinct inner and outer regions emerged, often accompanied by small inclusions or
182 domains within the droplet. These two-liquid morphologies typically adopted a core-shell geometry (Fig. 1),
183 consistent with LLPS criteria established in laboratory studies of mixed organic-inorganic particles, where phase
184 separation commonly occurs when moderately oxidized organics are mixed with inorganic salts such as AS or
185 AN (Song et al., 2013; You et al., 2013; Stewart et al., 2015; Kucinski et al., 2021; Huang et al., 2024).

186 Further dehydration to ~60% RH frequently produced three-phase morphologies. In this regime, solid-like
187 domains coexisted with two liquid regions. Some solid-like inclusions appeared angular (Fig. 1), suggesting
188 crystallized inorganic salts or less soluble organic materials. Based on the bulk ionic composition (dominated by
189 secondary inorganic salts such as AS; Fig. S2 and Sect. S1), it is plausible that at least part of the solid-like material
190 was inorganic-rich, though contributions from non-crystalline organic-rich phases cannot be excluded. The
191 relative volumes of the inner liquid, outer shell, and crystalline regions varied among droplets, reflecting
192 compositional differences and drying history. These observations align with recent laboratory studies showing
193 that mixed organic-inorganic aerosols can exhibit complex multiphase behavior across wide RH ranges (Huang
194 et al., 2021).

195 At low RH (~20 %), most droplets transitioned to non-liquid morphologies. Droplets displayed features
196 characteristic of efflorescence, either confined to the inner region or involving nearly the entire particle (Fig. 1).
197 These observations indicate that at least one phase had effectively lost its ability to flow, consistent with the
198 presence of effloresced inorganic solids and/or highly viscous organic material. Because morphology alone cannot
199 unambiguously distinguish crystalline solids from extremely viscous semisolids, these low-RH states are treated



200 qualitatively as non-liquid. Quantitative viscosity constraints are provided by poke-and-flow measurements in
 201 Sect. 3.3.



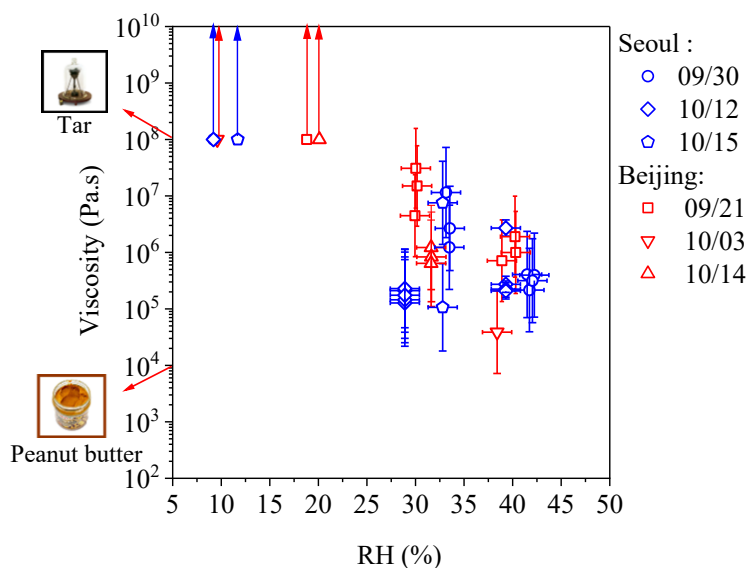
202
 203 **Figure 1. Optical images obtained during RH decrease for (a) Seoul and (b) Beijing PM_{2.5} droplets showing phase**
 204 **separation, as RH decreases from ~95% to 85, 60, and 20 %. Upon dehydration, particles transition from a**
 205 **homogeneous single phase to a core-shell morphology, illustrating separation of organic and inorganic components**
 206 **driven by water loss. The scale bar represents 20 μm. Seoul (10/15) and Beijing (10/14) samples have already been**
 207 **reported by Song et al. (2025) and are included here for completeness of discussion.**



208 3.3 Viscosity and phase state of organic-rich PM_{2.5}

209 To quantitatively constrain the RH-dependent viscosity of the organic-rich urban PM_{2.5}, we analyzed the $\tau_{(exp, flow)}$
210 obtained from the poke-and-flow experiments, with representative optical images shown in Fig. 3 and $\tau_{(exp, flow)}$
211 presented in (Fig. S1), in combination with fluid-dynamic simulations using COMSOL Multiphysics. Previous
212 field studies of ambient PM_{2.5} have primarily focused on qualitative phase-state classifications (e.g., liquid,
213 semisolid, or solid) (Bateman et al., 2016; Song et al., 2022; Meng et al., 2024; Seong et al., 2024). However,
214 quantitative, RH-resolved viscosity measurements for urban aerosols remain scarce.

215 Figure 2 shows the viscosities of PM_{2.5} droplets collected from Seoul and Beijing within the experimentally
216 accessible RH range (RH < ~40%). Across the RH range between ~40 and 25%, the mean viscosities were
217 approximately 10⁴–10⁸ Pa·s, corresponding to consistencies ranging from peanut butter to tar pitch (Koop et al.,
218 2011; Reid et al., 2018). Within the viscosity framework, the autumn-time urban PM_{2.5} droplets examined here
219 predominantly fell within the semisolid regime. The derived viscosities exhibited substantial sample-to-sample
220 and droplet-to-droplet variability, reflecting compositional heterogeneity and experimental uncertainty. The
221 overall uncertainty of individual viscosity estimates was within approximately two orders of magnitude, primarily
222 driven by assumptions regarding slip length in the fluid-dynamics simulations, as reported previously (Renbaum-
223 Wolff et al., 2013b; Grayson et al., 2015; Grayson et al., 2016).



224

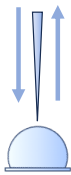
225 **Figure 2. Mean viscosities of PM_{2.5} droplets derived from experimentally measured flow times (Fig. S1) using poke-**
226 **and-flow measurements and COMSOL simulations. Markers denote mean values, with y-error bars indicating upper**
227 **and lower bound deviations from the mean, calculated as the difference between the mean and the corresponding upper**
228 **and lower bounds derived from simulations using minimum and maximum input parameters (Table S2). Upward**
229 **arrows indicate lower-limit viscosities where no restorative flow was observed within the experimental timescale. The**
230 **x-axis error bars represent the RH sensor uncertainty ($\pm 1.5\%$), as determined from our RH sensor calibration in the**
231 **flow cell. Reference viscosities for peanut butter ($\sim 10^4$ Pa·s) and tar ($\sim 10^8$ Pa·s) are shown for comparison (Koop et al.,**
232 **2011; Reid et al., 2018).**

233 At lower RH, PM_{2.5} droplets frequently exhibited brittle cracking without observable relaxation (Fig. 4).
234 When no restorative flow was detected over observation periods exceeding two hours, a conservative lower-limit
235 viscosity of $\sim 10^8$ Pa·s was assigned. Under these conditions, PM_{2.5} droplets from Seoul exhibited cracking at RH
236 values of $\sim 9.2\%$, $\sim 9.2\%$, and $\sim 11.7\%$, whereas droplets from Beijing cracked at comparatively higher and more

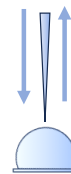


237 variable RH values of $\sim 18.8\%$, $\sim 9.6\%$, and $\sim 20.1\%$ on each date. These observations indicate that the RH
 238 threshold for the transition to non-flowing behavior is dependent on $PM_{2.5}$ composition. The inferred lower-bound
 239 viscosities correspond to consistencies comparable to, or exceeding, those of tar-like materials, suggesting
 240 extremely viscous properties or arrested internal flow under dry conditions.

(a) Seoul

date (mm/dd)	$PM_{2.5}$ ($\mu\text{g}/\text{m}^3$)	RH	pre-poking	poking	after poking	post poking
09/30	16.8	$\sim 40\%$			 $T = 0$	 $\tau_{exp,flow} = 97 \text{ s}$
10/12	16.4	$\sim 40\%$			 $T = 0$	 $\tau_{exp,flow} = 13 \text{ s}$
10/15	23.0	$\sim 33\%$			 $T = 0$	 $\tau_{exp,flow} = 48 \text{ s}$

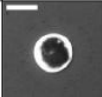
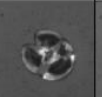
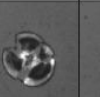
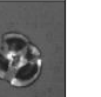
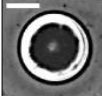
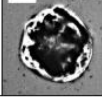
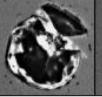
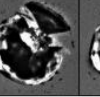
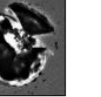
(b) Beijing

date (mm/dd)	$PM_{2.5}$ ($\mu\text{g}/\text{m}^3$)	RH	pre-poking	poking	after poking	post poking
09/21	16.5	$\sim 40\%$			 $T = 0$	 $\tau_{exp,flow} = 251 \text{ s}$
10/03	31.7	$\sim 40\%$			 $T = 0$	 $\tau_{exp,flow} = 15 \text{ s}$
10/14	7.0	$\sim 31\%$			 $T = 0$	 $\tau_{exp,flow} = 148 \text{ s}$

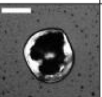
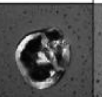
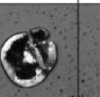
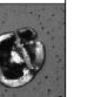
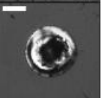
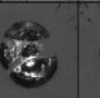
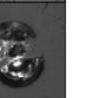
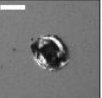
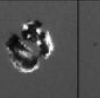
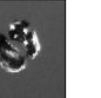
241
 242 **Figure 3. Poke-and-flow results for (a) Seoul and (b) Beijing $PM_{2.5}$ droplets at $\sim 40 - \sim 30\%$ RH conditions under which**
 243 **particle flow was observed. The post poking frame corresponds to the $\tau_{(exp, flow)}$, defined as the time required for the**
 244 **inner hole diameter to decrease to 50%. The scale bar represents 20 μm .**



(a) Seoul

date (mm/dd)	PM _{2.5} (μg/m ³)	RH	pre-poking	poking	after 0 sec	after 1 hr	after 2 hrs
09/30	16.8	~9.2%					
10/12	16.4	~9.2%					
10/15	23.0	~11.7%					

(b) Beijing

date (mm/dd)	PM _{2.5} (μg/m ³)	RII	pre-poking	poking	after 0 sec	after 1 hr	after 2 hrs
09/21	16.5	~18.8%					
10/03	31.7	~9.6%					
10/14	7.0	~20.1%					

245

246 **Figure 4. Optical images of (a) Seoul and (b) Beijing PM_{2.5} droplets exhibiting cracking at their respective RH after**
 247 **poking. The scale bar represents 20 μm.**

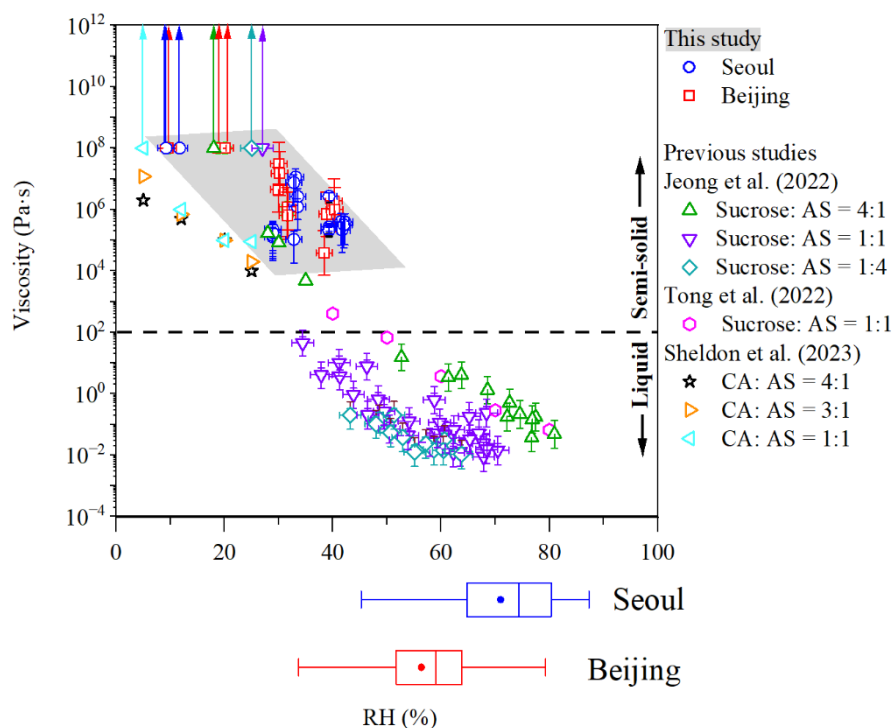
248 The autumn PM_{2.5} samples examined here were overall organic-rich, with sulfate as the dominant inorganic
 249 ion, primarily present as AS (Sect. 3.1). The RH-resolved viscosities measured for PM_{2.5} were compared with
 250 laboratory measurements for internally mixed organic–AS systems, commonly used as surrogates for organic-
 251 rich, sulfate-containing aerosols (Fig. 5). Previous laboratory studies indicated that citric acid (CA)–AS–H₂O
 252 systems exhibited relatively low viscosities and weak RH dependence at comparable RH, whereas sucrose–AS–
 253 H₂O systems showed a pronounced increase in viscosity upon dehydration, reaching ~10³–10⁵ Pa·s at RH of ~20–
 254 30% and approaching ~10⁸ Pa·s upon cracking at lower RH (e.g., sucrose–AS–H₂O for 4:1 and 1:1, Fig. 5) (Jeong



255 et al., 2022; Tong et al., 2022; Sheldon et al., 2023). Accordingly, sucrose–AS systems represent the highest RH-
256 dependent viscosities reported among commonly used laboratory surrogates, providing an appropriate upper
257 reference for comparison with organic-rich urban PM_{2.5}.

258 Within the experimentally accessible RH range ($\leq \sim 40\%$) in this study using the poke-and-flow technique, the
259 viscosities determined for organic-rich urban PM_{2.5} droplets were comparable to the highest values reported for
260 sucrose–AS laboratory systems and, in several cases, exceeded this upper range, while remaining consistently
261 higher than those reported for CA–AS systems at comparable RH. These results demonstrated that organic-rich
262 urban PM_{2.5} attained viscosities at the upper end of RH-dependent viscosity values previously reported for
263 laboratory-generated sucrose–AS–H₂O systems, without extrapolation beyond the measured RH range.

264 Our conclusions are based on a limited number of filters and droplets; broader seasonal and regional
265 generalizations will require more extensive sampling. In addition, because the experiments were conducted on
266 micrometer-sized extracted droplets on a substrate, future studies should combine rheological measurements with
267 phase-resolved chemical imaging and explicitly examine temperature dependence over a wider, atmospherically
268 relevant range to better constrain viscosity variability under real boundary-layer conditions.



269

270 **Figure 5.** RH-dependent viscosities of Beijing and Seoul PM_{2.5} droplets compared with sucrose–AS–H₂O and citric acid
271 (CA)–AS–H₂O systems from previous studies (Jeong et al., 2022; Tong et al., 2022; Sheldon et al., 2023). y-error bars
272 in this study indicate uncertainty ranges of the modeled viscosities for data corresponding to Fig. 2. Box plots in the
273 lower panel show hourly RH distributions in Seoul and Beijing derived from the days on which PM_{2.5} samples were
274 collected, with markers indicating mean values, boxes representing the 25th–75th percentiles, and whiskers showing
275 minimum and maximum values.

276 4. Conclusion

277 In this study, we investigated the phase behavior and viscosity of organic-rich urban PM_{2.5} collected during
278 autumn from Seoul and Beijing, using filter extracts. Optical microscopy observations revealed RH-driven phase
279 transitions, including well-mixed single liquid, two liquid phases, three phases, and the development of non-
280 flowing morphologies during dehydration. Using the poke-and-flow technique coupled with fluid-dynamic



281 simulations, we quantitatively constrained aerosol viscosity at ~ 290 K within the experimentally accessible RH
282 range ($\text{RH} < \sim 40\%$). For $\sim 40\text{--}25\%$ RH, the inferred viscosities of organic-rich $\text{PM}_{2.5}$ spanned approximately 10^4--
283 10^8 Pa·s, corresponding to semisolid to non-flowing behavior on the experimental timescale. At lower RH, brittle
284 cracking without observable relaxation was observed, and conservative lower-limit viscosities of $\sim 10^8$ Pa·s were
285 assigned.

286 When placed in the context of existing laboratory studies, the viscosities inferred for organic-rich urban $\text{PM}_{2.5}$
287 were comparable to the highest values reported for sucrose–AS– H_2O laboratory systems and, in several cases,
288 exceeded this upper range within the RH interval of $20\text{--}40\%$, while remaining consistently higher than those
289 reported for CA–AS systems at similar RH. These findings demonstrated that organic-rich urban $\text{PM}_{2.5}$ can attain
290 viscosities at the upper end of RH-dependent viscosity values previously reported for laboratory-generated
291 organic–inorganic aerosol surrogates, without reliance on extrapolation beyond the measured RH range.

292 Although these viscosity constraints were derived from micrometer-sized droplets prepared from $\text{PM}_{2.5}$ filter
293 extracts and therefore do not fully preserve the native morphology or size of ambient submicron particles, the
294 results provide direct, field-based quantitative benchmarks for aerosol viscosity under atmospherically relevant
295 low-RH conditions. Such highly viscous or effectively non-flowing states are expected to slow intra-particle
296 diffusion and internal mixing, with implications for gas–particle partitioning and multiphase chemical processing
297 in organic-rich urban aerosols. Future studies extending these measurements across additional seasons,
298 compositions, and particle sizes will be essential for further constraining the role of aerosol viscosity in urban
299 atmospheric processes.



300 **Author contributions**

301 Mijung Song: Conceptualization, Data curation, Funding acquisition, Software, Supervision, Writing–review &
302 editing. Atta Ullah: Data curation, Software, Writing–original draft, Writing–review & editing. Ji Yi Lee: Data
303 curation, Review & editing. Kyoung-Soon Jang: Data curation, Review & editing. Zhijun Wu: Data curation,
304 Review & editing.

305 **Funding Sources**

306 This work was supported by the National Research Foundation of Korea (NRF) grant funded by the Korea
307 government (MSIT) (RS-2024-00335536), by the Global Learning & Academic research institution for master’s
308 and PhD students, and Postdocs (LAMP) Program of the NRF grant funded by the Ministry of Education (No.
309 RS-2024-00443714).

310 **Notes**

311 The authors declare no competing financial interest.

312 **Acknowledgment**

313 We thank Daeun Kim for technical support.

314

315



316 **References**

- 317 Aiken, A. C., DeCarlo, P. F., Kroll, J. H., Worsnop, D. R., Huffman, J. A., Docherty, K. S., Ulbrich, I. M., Mohr,
318 C., Kimmel, J. R., Sueper, D., Sun, Y., Zhang, Q., Trimborn, A., Northway, M., Ziemann, P. J., Canagaratna, M.
319 R., Onasch, T. B., Alfarra, M. R., Prevot, A. S. H., Dommen, J., Duplissy, J., Metzger, A., Baltensperger, U., and
320 Jimenez, J. L.: O/C and OM/OC ratios of primary, secondary, and ambient organic aerosols with high-resolution
321 time-of-flight aerosol mass spectrometry, *Environ. Sci. Technol.*, 42, 4478–4485,
322 <https://doi.org/10.1021/es703009q>, 2008.
- 323 An, Y., Xu, J., Feng, L., Zhang, X., Liu, Y., Kang, S., Jiang, B., and Liao, Y.: Molecular characterization of
324 organic aerosol in the Himalayas: insight from ultra-high-resolution mass spectrometry, *Atmos. Chem. Phys.*, 19,
325 1115–1128, <https://doi.org/10.5194/acp-19-1115-2019>, 2019.
- 326 Bateman, A. P., Gong, Z., Liu, P., Sato, B., Cirino, G., Zhang, Y., Artaxo, P., Bertram, A. K., Manzi, A. O., and
327 Rizzo, L. V.: Sub-micrometre particulate matter is primarily in liquid form over Amazon rainforest, *Nat. Geosci.*,
328 9, 34–37, <https://doi.org/10.1038/ngeo2599>, 2016.
- 329 Bei, N. F., Xiao, B., Wang, R. N., Yang, Y. N., Liu, L., Han, Y. M., and Li, G. H.: Impacts of aerosol-radiation
330 and aerosol-cloud interactions on a short-term heavy-rainfall event - a case study in the Guanzhong Basin, China,
331 *Atmos. Chem. Phys.*, 25, 10931–10948, <https://doi.org/10.5194/acp-25-10931-2025>, 2025.
- 332 Berkemeier, T., Shiraiwa, M., Pöschl, U., and Koop, T.: Competition between water uptake and ice nucleation by
333 glassy organic aerosol particles, *Atmos. Chem. Phys.*, 14, 12513–12531, [https://doi.org/10.5194/acp-14-12513-](https://doi.org/10.5194/acp-14-12513-2014)
334 [2014](https://doi.org/10.5194/acp-14-12513-2014), 2014.
- 335 Cai, M., Yuan, B., Hu, W., Chenshuo, Y., Huang, S., Yang, S., Chen, W., Peng, Y., Deng, Z., Zhao, J., Chen, D.,
336 Sun, J., and Shao, M.: New insight into the formation and aging processes of organic aerosol from positive matrix
337 factorization (PMF) analysis of ambient FIGAERO-CIMS thermograms, *Atmos. Chem. Phys.*, 26, 769–788,
338 <https://doi.org/10.5194/acp-26-769-2026>, 2026.



- 339 Canagaratna, M. R., Jimenez, J. L., Kroll, J. H., Chen, Q., Kessler, S. H., Massoli, P., Hildebrandt Ruiz, L.,
340 Fortner, E., Williams, L. R., Wilson, K. R., Surratt, J. D., Donahue, N. M., Jayne, J. T., and Worsnop, D. R.:
341 Elemental ratio measurements of organic compounds using aerosol mass spectrometry: characterization, improved
342 calibration, and implications, *Atmos. Chem. Phys.*, 15, 253–272, <https://doi.org/10.5194/acp-15-253-2015>, 2015.
- 343 Chen, Q., Heald, C. L., Jimenez, J. L., Canagaratna, M. R., Zhang, Q., He, L. Y., Huang, X. F., Campuzano-Jost,
344 P., Palm, B. B., and Poulain, L.: Elemental composition of organic aerosol: The gap between ambient and
345 laboratory measurements, *Geophys. Res. Lett.*, 42, 4182–4189, <https://doi.org/10.1002/2015GL063693>, 2015.
- 346 Cheng, B., Alapaty, K., and Arunachalam, S.: Spatiotemporal trends in PM_{2.5} chemical composition in the
347 conterminous US during 2006–2020, *Atmos. Environ.*, 316, 120188,
348 <https://doi.org/10.1016/j.atmosenv.2023.120188>, 2024a.
- 349 Cheng, Y. L., Chen, L., Wu, H., Liu, J. Y., Ren, J. Y., and Zhang, F.: Wintertime fine aerosol particles composition
350 and its evolution in two megacities of southern and northern China, *Sci. Total Environ.*, 914,
351 <https://doi.org/10.1016/j.scitotenv.2023.120188>, 2024b.
- 352 Cheung, H. C., Chou, C. C. K., Lee, C. S. L., Kuo, W. C., and Chang, S. C.: Hygroscopic properties and cloud
353 condensation nuclei activity of atmospheric aerosols under the influences of Asian continental outflow and new
354 particle formation at a coastal site in eastern Asia, *Atmos. Chem. Phys.*, 20, 5911–5922,
355 <https://doi.org/10.5194/acp-20-5911-2020>, 2020.
- 356 Ciobanu, V. G., Marcolli, C., Krieger, U. K., Weers, U., and Peter, T.: Liquid–liquid phase separation in mixed
357 organic/inorganic aerosol particles, *J. Phys. Chem. A*, 113, 10966–10978, <https://doi.org/10.1021/jp905054d>,
358 2009.
- 359 Daellenbach, K. R., Kourtschev, I., Vogel, A. L., Bruns, E. A., Jiang, J., Petäjä, T., Jaffrezo, J. L., Aksoyoglu, S.,
360 Kalberer, M., Baltensperger, U., El Haddad, I., and Prévôt, A. S. H.: Impact of anthropogenic and biogenic sources
361 on the seasonal variation in the molecular composition of urban organic aerosols: a field and laboratory study



- 362 using ultra-high-resolution mass spectrometry, *Atmos. Chem. Phys.*, 19, 5973–5991, [https://doi.org/10.5194/acp-](https://doi.org/10.5194/acp-19-5973-2019)
363 [19-5973-2019](https://doi.org/10.5194/acp-19-5973-2019), 2019.
- 364 Daellenbach, K. R., Cai, J., Hakala, S., Dada, L., Yan, C., Du, W., Yao, L., Zheng, F., Ma, J., Ungeheuer, F.,
365 Vogel, A. L., Stolzenburg, D., Hao, Y., Liu, Y., Bianchi, F., Uzu, G., Jaffrezo, J.-L., Worsnop, D. R., Donahue,
366 N. M., and Kulmala, M.: Substantial contribution of transported emissions to organic aerosol in Beijing, *Nat.*
367 *Geosci.*, 17, 747–754, <https://doi.org/10.1038/s41561-024-01493-3>, 2024.
- 368 Davies, J. F. and Wilson, K. R.: Nanoscale interfacial gradients formed by the reactive uptake of OH radicals onto
369 viscous aerosol surfaces, *Chem. Sci.*, 6, 7020–7027, <https://doi.org/10.1039/c5sc02326b>, 2015.
- 370 El Haddad, I., Vienneau, D., Daellenbach, K. R., Modini, R., Slowik, J. G., Upadhyay, A., Vasilakos, P. N., Bell,
371 D., de Hoogh, K., and Prevot, A. S. H.: Opinion: How will advances in aerosol science inform our understanding
372 of the health impacts of outdoor particulate pollution?, *Atmos. Chem. Phys.*, 24, 11981–12011,
373 <https://doi.org/10.5194/acp-24-11981-2024>, 2024.
- 374 Freedman, M. A.: Phase separation in organic aerosol, *Chem. Soc. Rev.*, 46, 7694–7705,
375 <https://doi.org/10.1039/C6CS00783J>, 2017.
- 376 Freedman, M. A., Huang, Q., and Pitta, K. R.: Phase transitions in organic and organic/inorganic aerosol particles,
377 *Annu. Rev. Phys. Chem.*, 75, 257–281, <https://doi.org/10.1146/annurev-physchem-083122-115909>, 2024.
- 378 Gerrebos, N. G., Browning, L. P., Nikkho, S., Chartrand, E. R., Zaks, J., Wu, C., and Bertram, A. K.: Two-phase
379 morphology and drastic viscosity changes in biomass burning organic aerosol after hydroxyl radical aging,
380 *Environ. Sci. Atmos.*, <https://doi.org/10.1039/D5EA00084J>, 2025.
- 381 Gerrebos, N. G. A., Zaks, J., Gregson, F. K. A., Walton-Raaby, M., Meeres, H., Zigg, I., Zandberg, W. F., and
382 Bertram, A. K.: High viscosity and two phases observed over a range of relative humidities in biomass burning
383 organic aerosol from Canadian wildfires, *Environ. Sci. Technol.*, 58, 21716–21728,
384 <https://doi.org/10.1021/acs.est.4c09148>, 2024.



385 Gkatzelis, G. I., Hohaus, T., Tillmann, R., Gensch, I., Müller, M., Eichler, P., Xu, K. M., Schlag, P., Schmitt, S.
386 H., Yu, Z., Wegener, R., Kaminski, M., Holzinger, R., Wisthaler, A., and Kiendler-Scharr, A.: Gas-to-particle
387 partitioning of major biogenic oxidation products: a study on freshly formed and aged biogenic SOA, *Atmos.*
388 *Chem. Phys.*, 18, 12969–12989, <https://doi.org/10.5194/acp-18-12969-2018>, 2018.

389 Gou, Y., Xie, M., and Chen, J.: The phase state and viscosity of organic aerosol and related impacts on atmospheric
390 physicochemical processes: A review, *Atmos. Environ.*, 343, 120985,
391 <https://doi.org/10.1016/j.atmosenv.2024.120985>, 2025.

392 Grayson, J. W., Song, M., Sellier, M., and Bertram, A. K.: Validation of the poke-flow technique combined with
393 simulations of fluid flow for determining viscosities in samples with small volumes and high viscosities, *Atmos.*
394 *Meas. Tech.*, 8, 2463–2472, <https://doi.org/10.5194/amt-8-2463-2015>, 2015.

395 Grayson, J. W., Zhang, Y., Mutzel, A., Renbaum-Wolff, L., Böge, O., Kamal, S., Herrmann, H., Martin, S. T.,
396 and Bertram, A. K.: Effect of varying experimental conditions on the viscosity of α -pinene derived secondary
397 organic material, *Atmos. Chem. Phys.*, 16, 6027–6040, <https://doi.org/10.5194/acp-16-6027-2016>, 2016.

398 Guo, S., Hu, M., Zamora, M. L., Peng, J., Shang, D., Zheng, J., Du, Z., Wu, Z., Shao, M., Zeng, L., Molina, M.
399 J., and Zhang, R.: Elucidating severe urban haze formation in China, *Proc. Natl. Acad. Sci. U.S.A.*, 111, 17373–
400 17378, <https://doi.org/10.1073/pnas.1419604111>, 2014.

401 Hallquist, M., Wenger, J. C., Baltensperger, U., Rudich, Y., Simpson, D., Claeys, M., Dommen, J., Donahue, N.
402 M., George, C., Goldstein, A. H., Hamilton, J. F., Herrmann, H., Hoffmann, T., Iinuma, Y., Jang, M., Jenkin, M.
403 E., Jimenez, J. L., Kiendler-Scharr, A., Maenhaut, W., McFiggans, G., Mentel, T. F., Monod, A., Prévôt, A. S.
404 H., Seinfeld, J. H., Surratt, J. D., Szmigielski, R., and Wildt, J.: The formation, properties and impact of secondary
405 organic aerosol: current and emerging issues, *Atmos. Chem. Phys.*, 9, 5155–5236, [https://doi.org/10.5194/acp-9-](https://doi.org/10.5194/acp-9-5155-2009)
406 [5155-2009](https://doi.org/10.5194/acp-9-5155-2009), 2009.



- 407 Ham, S., Babar, Z. B., Lee, J. B., Lim, H. J., and Song, M.: Liquid–liquid phase separation in secondary organic
408 aerosol particles produced from α -pinene ozonolysis and α -pinene photooxidation with/without ammonia, *Atmos.*
409 *Chem. Phys.*, 19, 9321–9331, <https://doi.org/10.5194/acp-19-9321-2019>, 2019.
- 410 Hinks, M. L., Brady, M. V., Lignell, H., Song, M., Grayson, J. W., Bertram, A. K., Lin, P., Laskin, A., Laskin, J.,
411 and Nizkorodov, S. A.: Effect of viscosity on photodegradation rates in complex secondary organic aerosol
412 materials, *Phys. Chem. Chem. Phys.*, 18, 8785–8793, <https://doi.org/10.1039/C5CP05226B>, 2016.
- 413 Hodzic, A., Campuzano-Jost, P., Bian, H. S., Chin, M., Colarco, P. R., Day, D. A., Froyd, K. D., Heinold, B., Jo,
414 D. S., Katich, J. M., Kodros, J. K., Nault, B. A., Pierce, J. R., Ray, E., Schacht, J., Schill, G. P., Schroder, J. C.,
415 Schwarz, J. P., Sueper, D. T., Tegen, I., Tilmes, S., Tsigaridis, K., Yu, P. F., and Jimenez, J. L.: Characterization
416 of organic aerosol across the global remote troposphere: a comparison of ATom measurements and global
417 chemistry models, *Atmos. Chem. Phys.*, 20, 4607–4635, <https://doi.org/10.5194/acp-20-4607-2020>, 2020.
- 418 Hosny, N., Fitzgerald, C., Vyšniauskas, A., Athanasiadis, A., Berkemeier, T., Uygur, N., Pöschl, U., Shiraiwa,
419 M., Kalberer, M., and Pope, F.: Direct imaging of changes in aerosol particle viscosity upon hydration and
420 chemical aging, *Chem. Sci.*, 7, 1357–1367, <https://doi.org/10.1039/C5SC02959G>, 2016.
- 421 Hu, W., Hu, M., Hu, W.-W., Zheng, J., Chen, C., Wu, Y., and Guo, S.: Seasonal variations in high time-resolved
422 chemical compositions, sources, and evolution of atmospheric submicron aerosols in the megacity Beijing, *Atmos.*
423 *Chem. Phys.*, 17, 9979–10000, <https://doi.org/10.5194/acp-17-9979-2017>, 2017.
- 424 Huang, Q., Pitta, K. R., Constantini, K., Ott, E.-J. E., Zuend, A., and Freedman, M. A.: Experimental phase
425 diagram and its temporal evolution for submicron 2-methylglutaric acid and ammonium sulfate aerosol particles,
426 *Phys. Chem. Chem. Phys.*, 26, 2887–2894, <https://doi.org/10.1039/D3CP04411D> 2024.
- 427 Huang, R. J., Zhang, Y. L., Bozzetti, C., Ho, K. F., Cao, J. J., Han, Y. M., Daellenbach, K. R., Slowik, J. G., Platt,
428 S. M., Canonaco, F., Zotter, P., Wolf, R., Pieber, S. M., Bruns, E. A., Crippa, M., Ciarelli, G., Piazzalunga, A.,
429 Schwikowski, M., Abbaszade, G., Schnelle-Kreis, J., Zimmermann, R., An, Z. S., Szidat, S., Baltensperger, U.,



- 430 El Haddad, I., and Prévôt, A. S. H.: High secondary aerosol contribution to particulate pollution during haze events
431 in China, *Nature*, 514, 218–222, <https://doi.org/10.1038/nature13774>, 2014.
- 432 Huang, Y., Mahrt, F., Xu, S., Shiraiwa, M., Zuend, A., and Bertram, A. K.: Coexistence of three liquid phases in
433 individual atmospheric aerosol particles, *Proc. Natl. Acad. Sci. U.S.A.*, 118, e2102512118,
434 <https://doi.org/10.1073/pnas.2102512111> 2021.
- 435 Jeon, J., Chen, Y., Kim, H., and Kim, Y. P.: Influences of meteorology on emission sources and physicochemical
436 properties of particulate matter in Seoul, Korea during the heating period, *Atmos. Environ.*, 303, 119733,
437 <https://doi.org/10.1016/j.atmosenv.2023.119733>, 2023.
- 438 Jeong, R., Lilek, J., Zuend, A., Xu, R., Chan, M. N., Kim, D., Moon, H. G., and Song, M.: Viscosity and physical
439 state of sucrose mixed with ammonium sulfate droplets, *Atmos. Chem. Phys.*, 22, 8805–8817,
440 <https://doi.org/10.5194/acp-22-8805-2022>, 2022.
- 441 Jimenez, J. L., Canagaratna, M. R., Donahue, N. M., Prevot, A. S. H., Zhang, Q., Kroll, J. H., DeCarlo, P. F.,
442 Allan, J. D., Coe, H., Ng, N. L., Aiken, A. C., Docherty, K. S., Ulbrich, I. M., Grieshop, A. P., Robinson, A. L.,
443 Duplissy, J., Smith, J. D., Wilson, K. R., Lanz, V. A., Hueglin, C., Sun, Y. L., Tian, J., Laaksonen, A., Raatikainen,
444 T., Rautiainen, J., Vaattovaara, P., Ehn, M., Kulmala, M., Tomlinson, J. M., Collins, D. R., Cubison, M. J., E.,
445 Dunlea, J., Huffman, J. A., Onasch, T. B., Alfarra, M. R., Williams, P. I., Bower, K., Kondo, Y., Schneider, J.,
446 Drewnick, F., Borrmann, S., Weimer, S., Demerjian, K., Salcedo, D., Cottrell, L., Griffin, R., Takami, A.,
447 Miyoshi, T., Hatakeyama, S., Shimono, A., Sun, J. Y., Zhang, Y. M., Dzepina, K., Kimmel, J. R., Sueper, D.,
448 Jayne, J. T., Herndon, S. C., Trimborn, A. M., Williams, L. R., Wood, E. C., Middlebrook, A. M., Kolb, C. E.,
449 Baltensperger, U., and Worsnop, D. R.: Evolution of organic aerosols in the atmosphere, *Science*, 326, 1525–
450 1529, <https://doi.org/10.1126/science.1180353>, 2009.
- 451 Kanakidou, M., Seinfeld, J. H., Pandis, S. N., Barnes, I., Dentener, F. J., Facchini, M. C., Van Dingenen, R.,
452 Ervens, B., Nenes, A., Nielsen, C. J., Swietlicki, E., Putaud, J. P., Balkanski, Y., Fuzzi, S., Horth, J., Moortgat,



- 453 G. K., Winterhalter, R., Myhre, C. E. L., Tsigaridis, K., Vignati, E., Stephanou, E. G., and Wilson, J.: Organic
454 aerosol and global climate modelling: a review, *Atmos. Chem. Phys.*, 5, 1053–1123, [https://doi.org/10.5194/acp-](https://doi.org/10.5194/acp-5-1053-2005)
455 [5-1053-2005](https://doi.org/10.5194/acp-5-1053-2005), 2005.
- 456 Kiland, K. J., Mahrt, F., Peng, L., Nikkho, S., Zaks, J., Crescenzo, G. V., and Bertram, A. K.: Viscosity, glass
457 formation, and mixing times within secondary organic aerosol from biomass burning phenolics, *ACS Earth Space*
458 *Chem.*, 7, 1388–1400, <https://doi.org/10.1021/acsearthspacechem.3c00039>, 2023.
- 459 Kim, H., Zhang, Q., and Heo, J.: Influence of intense secondary aerosol formation and long-range transport on
460 aerosol chemistry and properties in the Seoul metropolitan area during spring time: results from KORUS-AQ,
461 *Atmos. Chem. Phys.*, 18, 7149–7168, <https://doi.org/10.5194/acp-18-7149-2018>, 2018.
- 462 Kim, H., Zhang, Q., Bae, G. N., Kim, J. Y., and Lee, S. B.: Sources and atmospheric processing of winter aerosols
463 in Seoul, Korea: insights from real-time measurements using a high-resolution aerosol mass spectrometer, *Atmos.*
464 *Chem. Phys.*, 17, 2009–2033, <https://doi.org/10.5194/acp-17-2009-2017>, 2017.
- 465 Kim, J. Y., Kim, Y. P., Yu, X., Yu, J., Wu, Z., Lee, H.-M., Song, M., Jang, K. S., Kim, C., Choi, N. R., and Lee,
466 J. Y.: Concentrations and formation pathways of nitrogen-containing organic compounds in PM_{2.5} from Seoul
467 and Beijing, *Environ. Res.*, 286, 122959, <https://doi.org/10.1016/j.envres.2025.122959>, 2025.
- 468 Kim, N., Kim, Y., Ghim, Y., Song, M., Kim, C., Jang, K., Lee, K., Shin, H., Jung, J., and Wu, Z.: Spatial
469 distribution of PM_{2.5} chemical components during winter at five sites in Northeast Asia: High temporal resolution
470 measurement study, *Atmos. Environ.*, 290, 119359, <https://doi.org/10.1016/j.atmosenv.2022.119359>, 2022.
- 471 Koop, T., Bookhold, J., Shiraiwa, M., and Pöschl, U.: Glass transition and phase state of organic compounds:
472 dependency on molecular properties and implications for secondary organic aerosols in the atmosphere, *Phys.*
473 *Chem. Chem. Phys.*, 13, 19238–19255, <https://doi.org/10.1039/c1cp22617g>, 2011.
- 474 Kucinski, T. M., Ott, E.-J. E., and Freedman, M. A.: Dynamics of liquid–liquid phase separation in submicrometer
475 aerosol, *J. Phys. Chem. A*, 125, 4446–4453, <https://doi.org/10.1021/acs.jpca.1c01985>, 2021.



- 476 Kuwata, M. and Martin, S. T.: Phase of atmospheric secondary organic material affects its reactivity, Proc. Natl.
477 Acad. Sci. U.S.A., 109, 17354–17359, <https://doi.org/10.1073/pnas.1209071109>, 2012.
- 478 Lam, H. K., Xu, R. S., Choczynski, J., Davies, J. F., Ham, D. W., Song, M. J., Zuend, A., Li, W. T., Tse, Y. L. S.,
479 and Chan, M. N.: Effects of liquid-liquid phase separation and relative humidity on the heterogeneous OH
480 oxidation of inorganic-organic aerosols: insights from methylglutaric acid and ammonium sulfate particles,
481 Atmos. Chem. Phys., 21, 2053–2066, <https://doi.org/10.5194/acp-21-2053-2021>, 2021.
- 482 Li, J., Forrester, S. M., and Knopf, D. A.: Heterogeneous oxidation of amorphous organic aerosol surrogates by
483 O, NO₃, and OH at typical tropospheric temperatures, Atmos. Chem. Phys., 20, 6055–6080,
484 <https://doi.org/10.5194/acp-20-6055-2020>, 2020.
- 485 Liu, J., Zhang, F., Ren, J., Chen, L., Zhang, A., Wang, Z., Zou, S., Xu, H., and Yue, X.: The evolution of aerosol
486 mixing state derived from a field campaign in Beijing: implications for particle aging timescales in urban
487 atmospheres, Atmos. Chem. Phys., 25, 5075–5086, <https://doi.org/10.5194/acp-25-5075-2025>, 2025.
- 488 Liu, S., Moffett, C. E., Vandergrift, G., Shrivastava, M., Cheng, Z., China, S., Nizkorodov, S. A., Zelenyuk, A.,
489 and Faiola, C. L.: Secondary organic aerosol from OH oxidation of acyclic terpenes is more viscous and less
490 volatile than that of their cyclic analogs, ACS ES&T Air, 3, 83–94, <https://doi.org/10.1021/acsestair.5c00226>,
491 2026.
- 492 Maclean, A. M., Smith, N. R., Li, Y., Huang, Y., Hettiyadura, A. P. S., Crescenzo, G. V., Shiraiwa, M., Laskin,
493 A., Nizkorodov, S. A., and Bertram, A. K.: Humidity-dependent viscosity of secondary organic aerosol from
494 ozonolysis of β -caryophyllene: measurements, predictions, and implications, ACS Earth Space Chem., 5, 305–
495 318, <https://doi.org/10.1021/acsearthspacechem.0c00296>, 2021.
- 496 Mahant, S., Iversen, E. M., Kasparoglu, S., Bilde, M., and Petters, M. D.: Direct measurement of the viscosity of
497 ternary aerosol mixtures, Environ. Sci. Atmos., 3, 595–607, <https://doi.org/10.1039/D2EA00160H>, 2023.



- 498 Manavi, S. E. I., Aktypis, A., Siouti, E., Skyllakou, K., Myriokefalitakis, S., Kanakidou, M., and Pandis, S. N.:
499 Atmospheric aerosol spatial variability: Impacts on air quality and climate change, *One Earth*, 8,
500 <https://doi.org/10.1016/j.oneear.2025.101237>, 2025.
- 501 Marshall, F. H., Berkemeier, T., Shiraiwa, M., Nandy, L., Ohm, P. B., Dutcher, C. S., and Reid, J. P.: Influence
502 of particle viscosity on mass transfer and heterogeneous ozonolysis kinetics in aqueous–sucrose–maleic acid
503 aerosol, *Phys. Chem. Chem. Phys.*, 20, 15560–15573, <https://doi.org/10.1039/C8CP01666F>, 2018.
- 504 McNeill, V. F.: Atmospheric aerosols: clouds, chemistry, and climate, *Annu. Rev. Chem. Biomol. Eng.*, 8, 427–
505 444, <https://doi.org/10.1146/annurevchembioeng-060816-101538>, 2017.
- 506 Meng, X., Wu, Z., Chen, J., Qiu, Y., Zong, T., Song, M., Lee, J., and Hu, M.: Particle phase state and aerosol
507 liquid water greatly impact secondary aerosol formation: insights into phase transition and its role in haze events,
508 *Atmos. Chem. Phys.*, 24, 2399–2414, <https://doi.org/10.5194/acp-24-2399-2024>, 2024.
- 509 Nault, B. A., Jo, D. S., McDonald, B. C., Campuzano-Jost, P., Day, D. A., Hu, W. W., Schroder, J. C., Allan, J.,
510 Blake, D. R., Canagaratna, M. R., Coe, H., Coggon, M. M., DeCarlo, P. F., Diskin, G. S., Dunmore, R., Flocke,
511 F., Fried, A., Gilman, J. B., Gkatzelis, G., Hamilton, J. F., Hanisco, T. F., Hayes, P. L., Henze, D. K., Hodzic, A.,
512 Hopkins, J., Hu, M., Huey, L. G., Jobson, B. T., Kuster, W. C., Lewis, A., Li, M., Liao, J., Nawaz, M. O., Pollack,
513 I. B., Peischl, J., Rappenglück, B., Reeves, C. E., Richter, D., Roberts, J. M., Ryerson, T. B., Shao, M., Sommers,
514 J. M., Walega, J., Warneke, C., Weibring, P., Wolfe, G. M., Young, D. E., Yuan, B., Zhang, Q., de Gouw, J. A.,
515 and Jimenez, J. L.: Secondary organic aerosols from anthropogenic volatile organic compounds contribute
516 substantially to air pollution mortality, *Atmos. Chem. Phys.*, 21, 11201–11224, [https://doi.org/10.5194/acp-21-](https://doi.org/10.5194/acp-21-11201-2021)
517 [11201-2021](https://doi.org/10.5194/acp-21-11201-2021) 2021.
- 518 Nikkho, S., Bai, B., Mahrt, F., Zaks, J., Peng, L., Kiland, K. J., Liu, P., and Bertram, A. K.: Secondary organic
519 aerosol from biomass burning phenolic compounds and nitrate radicals can be highly viscous over a wide relative
520 humidity range., *Environ. Sci. Technol.*, 58, 21702–21715, <https://doi.org/10.1021/acs.est.4c06235>, 2024.



- 521 Pöhlker, M. L., Pöhlker, C., Quaas, J., Mülmenstädt, J., Pozzer, A., Andreae, M. O., Artaxo, P., Block, K., Coe,
522 H., Ervens, B., Gallimore, P., Gaston, C. J., Gunthe, S. S., Henning, S., Herrmann, H., Krüger, O. O., McFiggans,
523 G., Poulain, L., Raj, S. S., Reyes-Villegas, E., Royer, H. M., Walter, D., Wang, Y., and Pöschl, U.: Global organic
524 and inorganic aerosol hygroscopicity and its effect on radiative forcing, *Nat. Commun.*, 14, 6139,
525 <https://doi.org/10.1038/s41467-023-41695-8>, 2023.
- 526 Qiu, Y., Wu, Z., Man, R., Zong, T., Liu, Y., Meng, X., Chen, J., Chen, S., Yang, S., and Yuan, B.: Secondary
527 aerosol formation drives atmospheric particulate matter pollution over megacities (Beijing and Seoul) in East
528 Asia, *Atmos. Environ.*, 301, 119702, <https://doi.org/10.1016/j.atmosenv.2023.119702>, 2023.
- 529 Rasool, Q. Z., Shrivastava, M., Liu, Y., Gaudet, B., and Zhao, B.: Modeling the impact of the organic aerosol
530 phase state on multiphase OH reactive uptake kinetics and the resultant heterogeneous oxidation timescale of
531 organic aerosol in the Amazon rainforest, *ACS Earth Space Chem.*, 7, 1009–1024,
532 <https://doi.org/10.1021/acsearthspacechem.2c00366>, 2023.
- 533 Reid, J. P., Bertram, A. K., Topping, D. O., Laskin, A., Martin, S. T., Petters, M. D., Pope, F. D., and Rovelli, G.:
534 The viscosity of atmospherically relevant organic particles, *Nat. Commun.*, 9, <https://doi.org/10.1038/s41467-018-03027-z>, 2018.
- 536 Renbaum-Wolff, L., Grayson, J., and Bertram, A.: New methodology for measuring viscosities in small volumes
537 characteristic of environmental chamber particle samples, *Atmos. Chem. Phys.*, 13, 791–802,
538 <https://doi.org/10.5194/acp-13-791-2013>, 2013a.
- 539 Renbaum-Wolff, L., Grayson, J. W., Bateman, A. P., Kuwata, M., Sellier, M., Murray, B. J., Shilling, J. E., Martin,
540 S. T., and Bertram, A. K.: Viscosity of α -pinene secondary organic material and implications for particle growth
541 and reactivity, *Proc. Natl. Acad. Sci. U.S.A.*, 110, 8014–8019, <https://doi.org/10.1073/pnas.1219548110>, 2013b.



- 542 Rovelli, G., Song, Y.-C., Maclean, A. M., Topping, D. O., Bertram, A. K., and Reid, J. P.: Comparison of
543 approaches for measuring and predicting the viscosity of ternary component aerosol particles, *Anal. Chem.*, 91,
544 5074–5082, <https://doi.org/10.1021/acs.analchem.8b05353>, 2019.
- 545 Seinfeld, J. H., Bretherton, C. S., Carslaw, K. S., Coe, H., DeMott, P. J., Dunlea, E. J., Feingold, G., Ghan, S. J.,
546 Guenther, A., Kahn, R. A., Kraucunas, I., Kreidenweis, S. M., Molina, M. J., Nenes, A., Penner, J. E., Prather, K.
547 A., Ramanathan, V., Ramaswamy, V., Rasch, P. J., Ravishankara, A. R., Rosenfeld, D., Stephens, G. L., and
548 Wood, R.: Improving our fundamental understanding of the role of aerosol–cloud interactions in the climate
549 system, *Proc. Natl. Acad. Sci. U.S.A.*, 113, 5781–5790, <https://doi.org/10.1073/pnas.1514043113>, 2016.
- 550 Seong, C., Kim, D., Jeong, R., Qiu, Y. T., Wu, Z. J., Lee, J. Y., Lee, K. Y., Ahn, J., Jang, K. S., Zuend, A., Kim,
551 C., Natsagdorj, A., and Song, M.: Influence of relative humidity and composition on PM phases in Northeast Asia,
552 *ACS Earth Space Chem.*, 8, 788–797, <https://doi.org/10.1021/acsearthspacechem.4c00019>, 2024.
- 553 Sheldon, C. S., Choczynski, J. M., Morton, K., Palacios Diaz, T., Davis, R. D., and Davies, J. F.: Exploring the
554 hygroscopicity, water diffusivity, and viscosity of organic–inorganic aerosols – a case study on internally-mixed
555 citric acid and ammonium sulfate particles, *Environ. Sci. Atmos.*, 3, 24–34, <https://doi.org/10.1039/d2ea00116k>,
556 2023.
- 557 Shiraiwa, M., Ammann, M., Koop, T., and Pöschl, U.: Gas uptake and chemical aging of semisolid organic aerosol
558 particles, *Proc. Natl. Acad. Sci. U.S.A.*, 108, 11003–11008, <https://doi.org/10.1073/pnas.1103045108>, 2011.
- 559 Smith, N. R., Crescenzo, G. V., Huang, Y., Hettiyadura, A. P. S., Siemens, K., Li, Y., Faiola, C. L., Laskin, A.,
560 Shiraiwa, M., Bertram, A. K., and Nizkorodov, S. A.: Viscosity and liquid–liquid phase separation in healthy and
561 stressed plant SOA, *Environ. Sci. Atmos.*, 1, 140–153, <https://doi.org/10.1039/D0EA00020E>, 2021.
- 562 Son, J.-Y., Lee, J.-T., Kim, K.-H., Jung, K., and Bell, M. L.: Characterization of fine particulate matter and
563 associations between particulate chemical constituents and mortality in Seoul, Korea, *Environ. Health Perspect.*,
564 120, 872, <https://doi.org/10.1289/ehp.1104316>, 2012.



- 565 Song, M., Marcolli, C., Krieger, U. K., Lienhard, D. M., and Peter, T.: Morphologies of mixed
566 organic/inorganic/aqueous aerosol droplets, *Faraday Discuss.*, 165, 289–316, <https://doi.org/10.1039/c3fd00049d>,
567 2013.
- 568 Song, M., Marcolli, C., Krieger, U. K., Zuend, A., and Peter, T.: Liquid-liquid phase separation in aerosol
569 particles: Dependence on O:C, organic functionalities, and compositional complexity, *Geophys. Res. Lett.*, 39,
570 19801–19801, <https://doi.org/10.1029/2012gl052807>, 2012.
- 571 Song, M., Liu, P. F., Hanna, S. J., Li, Y. J., Martin, S. T., and Bertram, A. K.: Relative humidity-dependent
572 viscosities of isoprene-derived secondary organic material and atmospheric implications for isoprene-dominant
573 forests, *Atmos. Chem. Phys.*, 15, 5145–5159, <https://doi.org/10.5194/acp-15-5145-2015>, 2015.
- 574 Song, M., Liu, P., Hanna, S. J., Zaveri, R. A., Potter, K. J., You, Y., Martin, S. T., and Bertram, A. K.: Relative
575 humidity-dependent viscosity of secondary organic material from toluene photo-oxidation and possible
576 implications for organic particulate matter over megacities, *Atmos. Chem. Phys.*, 16, 8817–8830,
577 <https://doi.org/10.5194/acp-16-8817-2016>, 2016a.
- 578 Song, M., Li, Y., Seong, C., Yang, H., Jang, K.-S., Wu, Z., Lee, J. Y., Matsuki, A., and Ahn, J.: Direct observation
579 of liquid–liquid phase separation and core–shell morphology of PM_{2.5} collected from three Northeast Asian cities
580 and implications for N₂O₅ hydrolysis, *ACS ES&T Air*, 2, 1079–1088, <https://doi.org/10.1021/acsestair.5c00043>,
581 2025.
- 582 Song, M., Maclean, A. M., Huang, Y., Smith, N. R., Blair, S. L., Laskin, J., Laskin, A., DeRieux, W.-S. W., Li,
583 Y., Shiraiwa, M., Nizkorodov, S. A., and Bertram, A. K.: Liquid-liquid phase separation and viscosity within
584 secondary organic aerosol generated from diesel fuel vapors, *Atmos. Chem. Phys.*, 19, 12515–12529,
585 <https://doi.org/10.5194/acp-19-12515-2019>, 2019.
- 586 Song, M., Jeong, R., Kim, D., Qiu, Y., Meng, X., Wu, Z., Zuend, A., Ha, Y., Kim, C., Kim, H., Gaikwad, S., Jang,
587 K.-S., Lee, J. Y., and Ahn, J.: Comparison of phase states of PM_{2.5} over megacities, Seoul and Beijing, and their



588 implications for particle size distribution, *Environ. Sci. Technol.*, 56, 17581–17590,
589 <https://doi.org/10.1021/acs.est.2c06377>, 2022.

590 Song, Y. C., Haddrell, A. E., Bzdek, B. R., Reid, J. P., Bannan, T., Topping, D. O., Percival, C., and Cai, C.:
591 Measurements and predictions of binary component aerosol particle viscosity, *J. Phys. Chem. A.*, 120, 8123–
592 8137, <https://doi.org/10.1021/acs.jpca.6b07835>, 2016b.

593 Stewart, D. J., Cai, C., Nayler, J., Preston, T. C., Reid, J. P., Krieger, U. K., Marcolli, C., and Zhang, Y. H.:
594 Liquid-liquid phase separation in mixed organic/inorganic single aqueous aerosol droplets, *J. Phys. Chem. A.*,
595 119, 4177–4190, <https://doi.org/10.1021/acs.jpca.5b01658>, 2015.

596 Su, H., Cheng, Y., and Pöschl, U.: New multiphase chemical processes influencing atmospheric aerosols, air
597 quality, and climate in the Anthropocene, *Acc. Chem. Res.*, 53, 2034–2043,
598 <https://doi.org/10.1021/acs.accounts.0c00246>, 2020.

599 Suda, S. R., Petters, M. D., Yeh, G. K., Strollo, C., Matsunaga, A., Faulhaber, A., Ziemann, P. J., Prenni, A. J.,
600 Carrico, C. M., Sullivan, R. C., and Kreidenweis, S. M.: Influence of functional groups on organic aerosol cloud
601 condensation nucleus activity, *Environ. Sci. Technol.*, 48, 10182–10190, <https://doi.org/10.1021/es502147y>,
602 2014.

603 Sun, J., Zhang, Q., Canagaratna, M. R., Zhang, Y., Ng, N. L., Sun, Y., Jayne, J. T., Zhang, X., Zhang, X., and
604 Worsnop, D. R.: Highly time- and size-resolved characterization of submicron aerosol particles in Beijing using
605 an Aerodyne Aerosol Mass Spectrometer, *Atmos. Environ.*, 44, 131–140,
606 <https://doi.org/10.1016/j.atmosenv.2009.03.020>, 2010.

607 Sun, Y., Luo, H., Li, Y., Zhou, W., Xu, W., Fu, P., and Zhao, D.: Atmospheric organic aerosols: online molecular
608 characterization and environmental impacts, *npj Clim. Atmos. Sci.*, 8, 305, [https://doi.org/10.1038/s41612-025-](https://doi.org/10.1038/s41612-025-01199-2)
609 [01199-2](https://doi.org/10.1038/s41612-025-01199-2), 2025.



- 610 Swietlicki, E., Hansson, H.-C., Hämeri, K., Svenningsson, B., Massling, A., McFiggans, G., McMurry, P. H.,
611 Petäjä, T., Tunved, P., and Gysel, M.: Hygroscopic properties of submicrometer atmospheric aerosol particles
612 measured with H-TDMA instruments in various environments—a review, *Tellus B: Chem. Phys. Meteorol.*, 60,
613 432–469, <https://doi.org/10.1111/j.1600-0889.2008.00350.x>, 2008.
- 614 Tan, F., Zhang, H., Xia, K., Jing, B., Li, X., Tong, S., and Ge, M.: Hygroscopic behavior and aerosol chemistry
615 of atmospheric particles containing organic acids and inorganic salts, *npj Clim. Atmos. Sci.*, 7, 203,
616 <https://doi.org/10.1038/s41612-024-00752-9>, 2024.
- 617 Tao, J., Zhang, L., Cao, J., and Zhang, R.: A review of current knowledge concerning PM 2.5 chemical
618 composition, aerosol optical properties and their relationships across China, *Atmos. Chem. Phys.*, 17, 9485–9518,
619 <https://doi.org/10.5194/acp-17-9485-2017>, 2017.
- 620 Tong, Y.-K., Liu, Y., Meng, X., Wang, J., Zhao, D., Wu, Z., and Ye, A.: The relative humidity-dependent viscosity
621 of single quasi aerosol particles and possible implications for atmospheric aerosol chemistry, *Phys. Chem. Chem.*
622 *Phys.*, 24, 10514–10523, <https://doi.org/10.1039/d2cp00740a>, 2022.
- 623 Ullmann, D. A., Hinks, M. L., Maclean, A. M., Butenhoff, C. L., Grayson, J. W., Barsanti, K., Jimenez, J. L.,
624 Nizkorodov, S. A., Kamal, S., and Bertram, A. K.: Viscosities, diffusion coefficients, and mixing times of intrinsic
625 fluorescent organic molecules in brown limonene secondary organic aerosol and tests of the Stokes–Einstein
626 equation, *Atmos. Chem. Phys.*, 19, 1491–1503, <https://doi.org/10.5194/acp-19-1491-2019>, 2019.
- 627 Wall, C. J., Norris, J. R., Possner, A., McCoy, D. T., McCoy, I. L., and Lutsko, N. J.: Assessing effective radiative
628 forcing from aerosol-cloud interactions over the global ocean, *Proc. Natl. Acad. Sci. U.S.A.*, 119,
629 <https://doi.org/10.1073/pnas.2210481119>, 2022.
- 630 World Health Organization: WHO global air quality guidelines: particulate matter (PM_{2.5} and PM₁₀), ozone,
631 nitrogen dioxide, sulfur dioxide and carbon monoxide, Geneva, 2021.



- 632 You, Y., Renbaum-Wolff, L., and Bertram, A. K.: Liquid-liquid phase separation in particles containing organics
633 mixed with ammonium sulfate, ammonium bisulfate, ammonium nitrate or sodium chloride, *Atmos. Chem. Phys.*,
634 13, 11723–11734, <https://doi.org/10.5194/acp-13-11723-2013>, 2013.
- 635 Zaveri, R. A., Shilling, J. E., Zelenyuk, A., Zawadowicz, M. A., Suski, K., China, S., Bell, D. M., Veghte, D., and
636 Laskin, A.: Particle-phase diffusion modulates partitioning of semivolatile organic compounds to aged secondary
637 organic aerosol, *Environ. Sci. Technol.*, 54, 2595–2605, <https://doi.org/10.1021/acs.est.9b05514>, 2020.
- 638 Zhang, J., Su, Y., Chen, C., Guo, W., Tan, Q., Feng, M., Song, D., Jiang, T., Chen, Q., Li, Y., Li, W., Wang, Y.,
639 Huang, X., Han, L., Wu, W., and Wang, G.: Chemical composition, sources and formation mechanism of urban
640 PM_{2.5} in Southwest China: a case study at the beginning of 2023, *Atmos. Chem. Phys.*, 24, 2803–2820,
641 <https://doi.org/10.5194/acp-24-2803-2024>, 2024.
- 642 Zhang, Q., Jimenez, J. L., Canagaratna, M. R., Allan, J. D., Coe, H., Ulbrich, I., Alfarra, M. R., Takami, A.,
643 Middlebrook, A. M., Sun, Y. L., Dzepina, K., Dunlea, E., Docherty, K., DeCarlo, P. F., Salcedo, D., Onasch, T.,
644 Jayne, J. T., Miyoshi, T., Shimonono, A., Hatakeyama, S., Takegawa, N., Kondo, Y., Schneider, J., Drewnick, F.,
645 Borrmann, S., Weimer, S., Demerjian, K., Williams, P., Bower, K., Bahreini, R., Cottrell, L., Griffin, R. J.,
646 Rautiainen, J., Sun, J. Y., Zhang, Y. M., and Worsnop, D. R.: Ubiquity and dominance of oxygenated species in
647 organic aerosols in anthropogenically-influenced Northern hemisphere midlatitudes, *Geophys. Res. Lett.*, 34,
648 <https://doi.org/10.1029/2007GL029979>, 2007.
- 649 Zhang, Y., Tang, L., Croteau, P., Favez, O., Sun, Y., Canagaratna, M. R., Wang, Z., Couvidat, F., Albinet, A.,
650 Zhang, H., Sciare, J., Prévôt, A. S. H., Jayne, J. T., and Worsnop, D. R.: Field characterization of the PM 2.5
651 Aerosol Chemical Speciation Monitor: insights into the composition, sources, and processes of fine particles in
652 eastern China, *Atmos. Chem. Phys.*, 17, 14501–14517, <https://doi.org/10.5194/acp-17-14501-2017>, 2017.
- 653 Zhao, J., Qiu, Y. M., Zhou, W., Xu, W. Q., Wang, J. F., Zhang, Y. J., Li, L. J., Xie, C. H., Wang, Q. Q., Du, W.,
654 Worsnop, D. R., Canagaratna, M. R., Zhou, L. B., Ge, X. L., Fu, P. Q., Li, J., Wang, Z. F., Donahue, N. M., and



- 655 Sun, Y. L.: Organic aerosol processing during winter severe haze episodes in Beijing, *J. Geophys. Res. Atmos.*,
656 124, 10248–10263, <https://doi.org/10.1029/2019jd030832>, 2019.
- 657 Zhou, S., Shiraiwa, M., McWhinney, R. D., Pöschl, U., and Abbatt, J. P.: Kinetic limitations in gas-particle
658 reactions arising from slow diffusion in secondary organic aerosol, *Faraday Discuss.*, 165, 391–406,
659 <https://doi.org/10.1039/C3FD00030C>, 2013.
- 660 Zhou, W., Xu, W., Kim, H., Zhang, Q., Fu, P., Worsnop, D. R., and Sun, Y.: A review of aerosol chemistry in
661 Asia: insights from aerosol mass spectrometer measurements, *Environ. Sci. Process. Impacts*, 22, 1616–1653,
662 <https://doi.org/10.1039/D0EM00212G>, 2020.
- 663 Zobrist, B., Marcolli, C., Pedernera, D. A., and Koop, T.: Do atmospheric aerosols form glasses?, *Atmos. Chem.*
664 *Phys.*, 11, 10823–10837, <https://doi.org/10.5194/acp-8-5221-2008>, 2011.
- 665 Zuend, A. and Seinfeld, J. H.: Modeling the gas-particle partitioning of secondary organic aerosol: the importance
666 of liquid-liquid phase separation, *Atmos. Chem. Phys.*, 12, 3857–3882, [https://doi.org/10.5194/acp-12-3857-](https://doi.org/10.5194/acp-12-3857-2012)
667 [2012](https://doi.org/10.5194/acp-12-3857-2012), 2012.
- 668